# High Temperature Lifetime of Polyimide/Poly(silsesquioxane)-like Hybrid Films

**Mei-Hui Tsai and Wha-Tzong Whang***

*Department of Materials Science and Engineering, National Chiao Tung University, Hsinchu 30049, Taiwan, ROC*

Received February 16, 2001; revised April 13,2001; accepted April 20, 2001.

**Abstract:** Decomposition kinetics in thermogravimetric analysis (TGA) and dynamic mechanical relaxation in dynamic mechanical analysis (DMA) are used to study the high temperature lifetime of the new type of polyimide/poly(silsesquioxane)-like (PI/PSSQ-like) hybrid films, which are designed to form three-dimensional structures with linear polyimide blocks and a crosslinked PSSQ-like structure. Both TGA and DMA analysis reveal that the PI/PSSQ-like hybrid films have a longer lifetime (are more reliable) with regard to their thermal and mechanical characteristics than that of pure PI. Even just 2 wt% of *p*-aminophenyltrimethoxysilane (APTS) in a PI/PSSQ-like hybrid film can significantly improve the service lifetime by as much as at least four times in a TGA decomposition kinetic study. The dynamical relaxation data are well fitted to the calculated WLF (Williams-Landel-Ferry) master curves. In a series of X-PIS (PI modified with APTS) hybrid films, decreasing the PI block chain length increases the decomposition activation energy, lifetime (in both TGA and DMA) and relaxation modulus. In a series of X-PIS-y-PTS [PI modified with APTS and phenyltrimethoxysilane (PTS)] films, the decomposition activation energy and lifetime (in TGA) increase with the PTS content. Interestingly, the dynamic mechanical relaxation modulus of 10000-PIS-100-PTS film is lower than that of the corresponding 10000-PIS film at frequency > $10^2$ rad/sec, but higher at frequency < $10^2$ rad/sec. The 10000-PIS-100-PTS has a lower relaxation time than the 10000-PIS at the modulus $5\times10^8$ Pa, but the relaxation time of the former becomes higher at $5\times10^7$ Pa .

Keywords: Polyimide/poly(silsesquioxane)-like, Decomposition activation energy, Master curve, WLF equation, Dynamic relaxation modulus, Lifetime.

## Introduction

In the past three decades, polyimides have been used as reliable high-temperature polymers [1-4]. They have been widely utilized as packaging materials and dielectric layers for the electronic and microelectronic industry because of their outstanding characteristics, such as a low dielectric constant [5-9], excellent mechanical properties and high thermal stability [2,4]. Poly(silsesquioxane) (PSSQ) has been used as a low dielectric material in integrated circuit chips [10-12]. In order to maintain a low dielectric constant as well as excellent thermal stability and mechanical strength, PI/PSSQ-like hybrid films are successfully prepared from hybridizing linear PI blocks with PSSQ-like crosslink structures [13-29]. The PI/PSSQ-like hybrid films may also have high optical transparency as well as a low moisture absorption and thermal expansion coefficient [13,14]. The material for microelectronic applications must be able to meet the high-temperature processing requirements, including sealing, packaging, die bonding, wire bonding, and soldering [1].

The ability to predict the service lifetime of the material is very important in microelectronic applications. Thermogravimetric analysis (TGA) provides a method of accelerating the lifetime test of polymers so that short-time experiments can be used

*To whom all correspondence should be addressed.
Tel: 886-3-5731873; Fax: 886-3-5724727
E-mail: wtwhang@cc.nctu.edu.tw

J. Polym. Res. is covered in ISI (CD, D, MS, Q, RC, S), CA, EI, and Polymer Contents.

**Table I.** The compositions of APTS-PAA with 25 % solid content in 15 g of NMP solvent.

| APTS-PAA / X[a]-PIS | Composition in mole × $10^3$ (g) | | | APTS (wt%)[b] | DMA $T_g$[c] (°C) |
|---|---|---|---|---|---|
| | ODPA | ODA | APTS | | |
| 3000-PIS | 9.057 (2.8096) | 7.390 (1.4802) | 6.659 (0.7102) | 14.20 | 289 |
| 5000-PIS | 9.352 (2.9011) | 8.352 (1.6724) | 2.000 (0.4265) | 8.53 | 287 |
| 10000-PIS | · 9.573 (2.9698) | 9.075 (1.8171) | 4.995 (0.2131) | 4.26 | 284 |
| 15000-PIS | 9.647 (2.9927) | 9.314 (1.8652) | 0.666 (0.1421) | 2.84 | 279 |
| 20000-PIS | 9.684 (3.0043) | 9.437 (1.8892) | 0.500 (0.1065) | 2.13 | 277 |
| Pure PI | 9.795 (3.0385) | 9.795 (1.9615) | 0.000 (0.0000) | 0 | 270 |

(a) Molecular weight of polyimide block chain length.
(b) Weight percentage of APTS in APTS-PAA solid.
(c) $T_g$ of the pure PI and X-PIS measured by DMA at 1 Hz.

to predict in-use lifetime. In the TGA decomposition kinetic study, the material is heated at several different heating rates through its decomposition region. The high temperature lifetime [1,30-32] for a specific decomposition level can be determined from the resultant thermal curves.

The linear viscoelastic properties of polymers are both time and temperature dependent. Performing frequency-multiplexing experiments on a dynamical mechanical analyzer (DMA) at different frequencies enables collection of the viscoelastic data. The polyimide stress relaxation master curves [33,34] together with physical aging shift factor [35-37] can be used to establish time-temperature dependent behavior and to predict long-term response. Time-temperature superposition is applied to predict the long-term properties of polymers based on short-time tests [38-41]. Usually, the dynamic mechanical relaxation time is used as the mechanical lifetime of the material at the specific condition.

The dynamic mechanical properties of PI/PSSQ-like hybrid films and the low dielectric of PI/PSSQ-like nanocomposite materials have been discussed in other papers [13,14]. In this study, we focus on the high temperature lifetime of PI/PSSQ-like hybrid films because a systematic study on long-term reliability in the PI/PSSQ-like hybrid films is not available. In this article, we intend to correlate the properties with the silica component, the PSSQ-like content and the PI block chain length. The influences of composition, time, and temperature on the decomposition activation energy, thermal lifetime, mechanical relaxation time and relaxation processes are studied with TGA and DMA.

## Experimental

### 1. Materials

4,4'-Diaminodiphenylether (ODA, 98%) from Lancaster was dried in a vacuum oven at 120 °C for 3 hours prior to use. 3,3'-Oxydiphthalic anhydride (ODPA, 98%) from Tokyo Chemical Industry was purified by recrystallization from acetic anhydride and dried in a vacuum oven at 125 °C overnight. *N*-methyl-2-pyrrolidone (NMP) from Tedia Company was dehydrated with molecular sieves. *p*-Aminophenyl-trimethoxysilane (APTS, 95% para and 5% meta) from Gelest Inc. and phenyltrimethoxysilane (PTS, 98%) from Lancaster were used as supplied.

### 2. Preparation of aminophenyltrimethoxysilyl-terminated poly(amic acid) (APTS-PAA) and poly(amic acid)phenyltrimethoxysilane (PAA-PTS)

Polycondensation was carried out in a flask by adding a diamine ODA, a monoamine APTS and a dianhydride ODPA in NMP under nitrogen stream at room temperature. APTS was used to control the chain length of the trimethoxysilyl-terminated polyamic acid. In the preparation of the APTS-terminated PAA with a PAA block molecular weight of 5,000, 0.04676 moles of ODPA was added into the solution containing 0.04176 moles of ODA and 0.01 moles of APTS in 75 g of NMP. ODPA was introduced into the solution in five portions. After the dissolution of all the ODPA, the reaction mixture was further stirred for 2 hours at room temperature. The PAA solution had 25 % solid content (w/w). Other APTS-PAAs with different PAA

**Table II.** The compositions of PAA-PTS solutions in 15 g of NMP solvent.

| PAA-PTS / X-PIS-y-PTS | Composition in mole × $10^3$ | | | PTS (g) | $Y^{(a)}$ | DMA $T_g^{(b)}$ (°C) |
|---|---|---|---|---|---|---|
| | ODPA | ODA | APTS | | | |
| 5000-PIS-24-PTS | 9.352 (2.9011) | 8.352 (1.6724) | 2.000 (0.4265) | 1.2 | 24 | 283 |
| 5000-PIS-50-PTS | 9.352 (2.9011) | 8.352 (1.6724) | 2.000 (0.4265) | 2.5 | 50 | 281 |
| 5000-PIS-70-PTS | 9.352 (2.9011) | 8.352 (1.6724) | 2.000 (0.4265) | 3.5 | 70 | 279 |
| 5000-PIS-100-PTS | 9.352 (2.9011) | 8.352 (1.6724) | 2.000 (0.4265) | 5.0 | 100 | 277 |
| 5000-PIS-140-PTS | 9.352 (2.9011) | 8.352 (1.6724) | 2.000 (0.4265) | 7.0 | 140 | 273 |
| 10000-PIS-100-PTS | 9.573 (2.9698) | 9.075 (1.8171) | 4.995 (0.2131) | 5.0 | 100 | 281 |

(a) Weight ratio (%) of PTS to APTS-PAAs.
(b) $T_g$ of the X-PIS-y-PTS measured by DMA at 1 Hz.

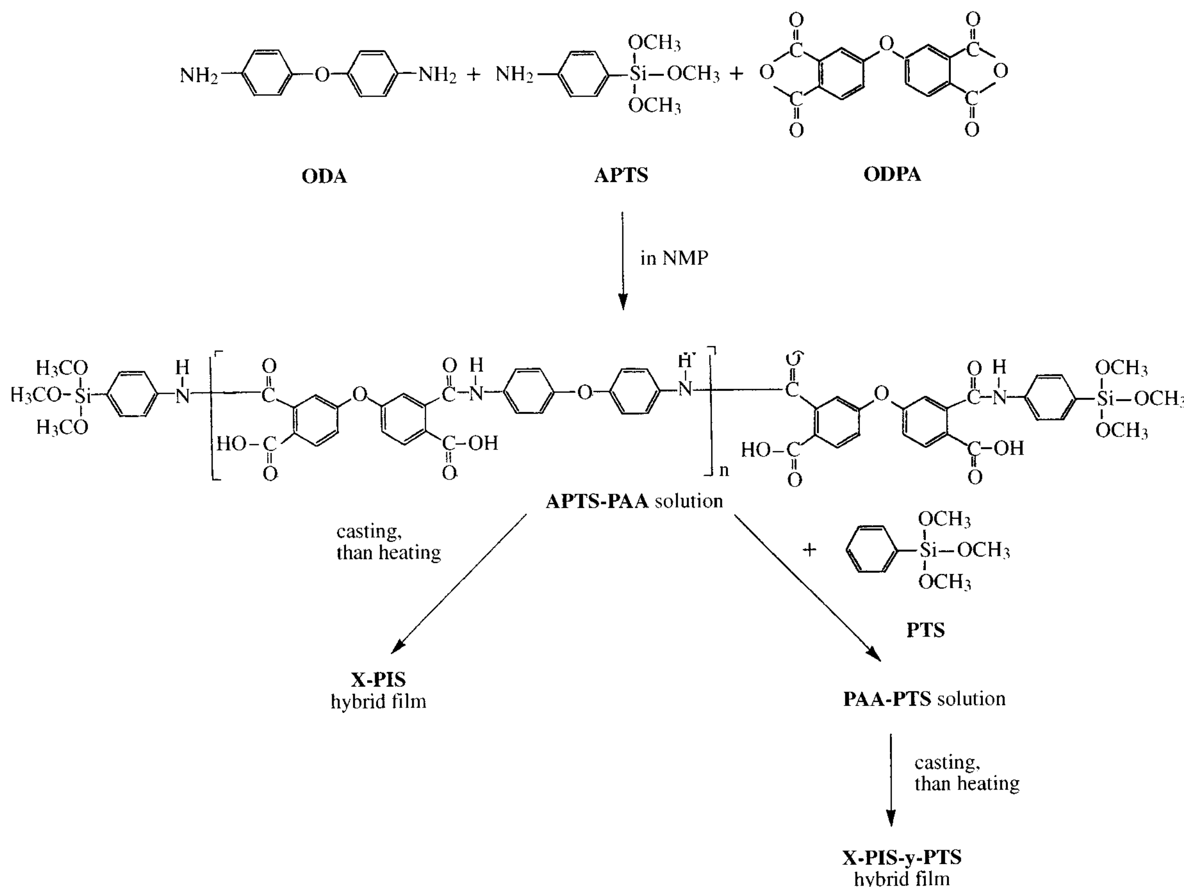


Scheme 1

block lengths were also prepared in the same way. The compositions of APTS-PAAs are listed in Table I.

The APTS-PAA solution stated above was divided into several equal portions (20 g solution for each). Different weights of PTS were added to each portion to get PAA-PTS solutions. Stirring was continued at room temperature for 15 hours to give a

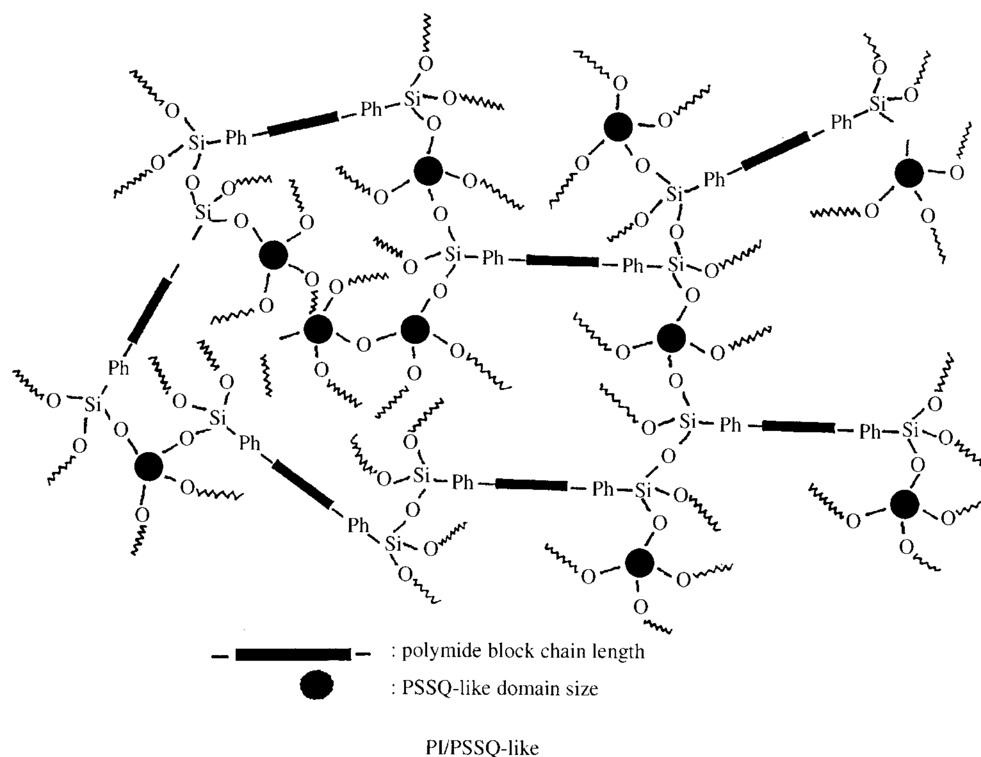


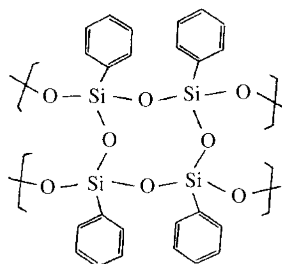

PSSQ

**Scheme 2**

homogenous PAA-PTS solution. The compositions of PAA-PTS are listed in Table II.

### 3. Preparation of polyimide/poly(silsesquioxane)-like (PI/PSSQ-like) hybrid films

APTS-PAA and PAA-PTS solutions were cast on glass plates with a thickness of 250 μm, placed at room temperature for 40 minutes, then step heated for one hour at 60 °C each of the following temperatures, 100, 150, 200 and 300 °C, to obtain PI/PSSQ-like films. The thickness of the PI/PSSQ-like films from APTS-PAA and PAA-PTS ranged from 30 to 50 μm. The PI/PSSQ-like hybrid films from APTS-PAA and PAA-PTS film are encoded as X-PIS and X-PIS-y-PTS respectively, where X is the molecular weight of each polyimide block and y is the weight ratio percentage of PTS to APTS-PAA (solid/solid). Their $T_g$s are listed in Tables I and II, respectively. The reaction procedure schematic is shown in Scheme 1, and PSSQ and PI/PSSQ-like structures are shown in Scheme 2.

### 4. Characterization

Thermogravimetric analysis (TGA) decomposition kinetics was carried out with a TA Instruments TGA 2950 at heating rates of 1, 5, 10, and 20 °C/min from 80-800 °C under atmosphere. The tested sample was weighted as 10 mg. The hybrid films were first heated at 110 °C for 3 hours in a forced air convection oven to remove any water and to reach the initial weight of the hybrid films before measuring. The lifetime curves and decomposition

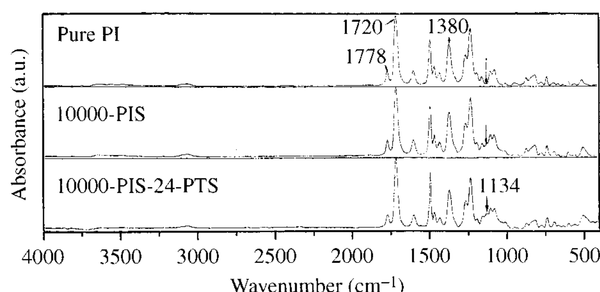


**Figure 1.** Infrared spectra of pure ODA-ODPA polyimide, 10000-PIS and 10000-PIS-24-PTS.

activation energies were obtained by analyzing the dynamic TGA data with the TGA decomposition kinetics software provided by TA Instruments. The glass transition temperature (tanδ peak) measurements and dynamic mechanical relaxation experiments were performed using a TA Instruments DMA 2980 Dynamic Mechanical Analyzer. The $T_g$ was determined at a heating rate of 3 °C/min from 60 to 350 °C and at a frequency of 1 Hz. The relaxation modulus was measured as a function of frequency and temperature. The temperature range was measured from well below $T_g$ to about ($T_g$+40) °C. The multi frequency scans (20, 10, 5, 1, 0.5, and 0.1 Hz) were run at a step heating rate of 2 °C/min from 240 to 310-330 °C with a tension clamp to hold the sample (15×5 mm). The master curves of the PI/PSSQ-like hybrid films were obtained using the TA Instruments DMA time-temperature superposition software.

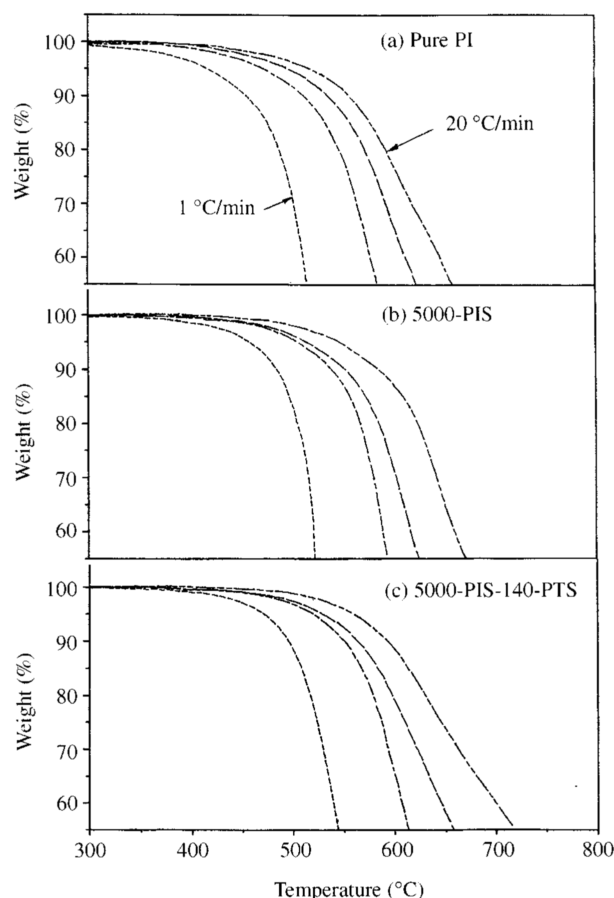


**Figure 2.** Dynamic TGA curves of (a) pure PI, (b) 5000-PIS, and (c) 5000-PIS-140-PTS hybrid films at heating rates of 1, 5, 10 and 20 °C/min under atmosphere. 1 (- - -), 5 (— -), 10 (— —), and 20 (— - -) °C/min.

## Results and Discussion

Polyimide/poly(silsesquioxane)-like hybrid film is a novel material. Figure 1 shows the infrared spectra of pure ODA-ODPA polyimide, 10000-PIS and 10000-PIS-24-PTS. The asymmetric and symmetric carbonyl stretch of the imide ring at 1778 and 1720 $cm^{-1}$ and the C-N stretch at 1380 $cm^{-1}$ are all characteristic of the polyimide. The increase in the absorption band at 1110-1140 $cm^{-1}$ in the spectra of 10000-PIS and 10000-PIS-24-PTS films is due to Si-O-Si bond formation in the sol-gel process. Systematic studies on their dynamic mechanical properties as well as their dielectric and synthesis characteristics correlated with their chemical composition and physical structure have been reported in our previous papers [13,14]. In this paper we study the high temperature lifetime of PI/PSSQ-like hybrid films.

Figure 2 displays the dynamic thermogravimetric curves of pure PI, 5000-PIS, and 5000-PIS-140-PTS hybrid films at various heating rates of 1, 5, 10, 20 °C/min under atmosphere. All polymer films exhibit one-step decomposition. Thermal decomposition often follows the Arrhenius kinetics model [30]:

$$d\alpha/dt = f(\alpha)[Z \exp(-E_a/RT)] \quad (1)$$

Where α is the fraction of weight loss, f(α) a function of α and independent of temperature, Z the pre-exponential factor, $E_a$ the activation energy, R the universal gas constant, t the time and T the temperature in K. At a constant heating rate, $d\alpha/dt = d\alpha/dT \times \beta]$, where β is the heating rate. By plotting the logarithmic heating rate against the temperature reciprocal at a particular weight loss (conversion %) for several heating rates, the activation energy can be found from the slope of the best-fit line. Figure 3 shows the logarithmic heating rate against the temperature reciprocal at 1%, 2.5%, and 5% weight loss of 5000-PIS films. By using the Flynn method [30],

**Table III.** Decomposition activation energies of pure ODA-ODPA polyimide, X-PIS and X-PIS-y-PTS hybrid films with different conversion level.

| Sample code \ Conversion (wt%) \ $E_a$ | Activation energy (KJ/mole) | | |
|---|---|---|---|
| | 1% | 2.5% | 5% |
| 3000-PIS | 231 | 247 | 268 |
| 5000-PIS | 197 | 224 | 253 |
| 10000-PIS | 164 | 195 | 246 |
| 20000-PIS | 144 | 165 | 193 |
| Pure PI | 111 | 129 | 174 |
| 5000-PIS-70-PTS | 209 | 230 | 259 |
| 5000-PIS-140-PTS | 234 | 240 | 269 |

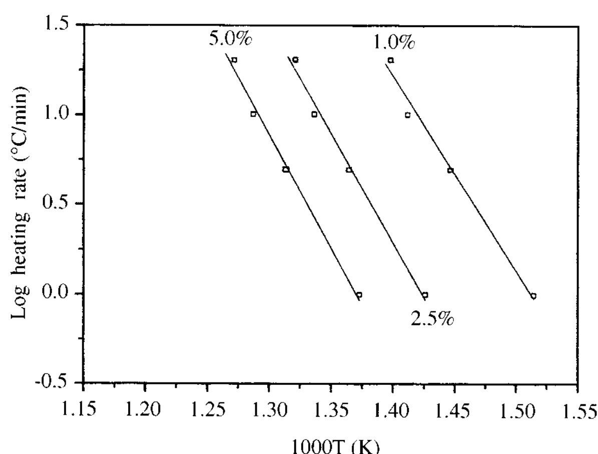


Figure 3. Relationship between logarithmic heating rate and reciprocal temperature of 3000-PIS.

the decomposition activation energy can be obtained. Table III shows the decomposition activation energy of pure ODA-ODPA polyimide and the X-PIS and X-PIS-y-PTS hybrid films at 1%, 2.5% and 5% weight loss. A low level of weight loss is used to characterize the materials for microelectronic applications because high reliability is required. It shows that the activation energies increase with the weight loss percentage in the same polyimides, the lowest $E_a$ in 1% conversion and the highest $E_a$ in 5% conversion. In the X-PIS series, the activation energy in the same conversion increases with decreasing the PI block length. In the 5000-PIS-y-PTS series, incorporating PTS into the hybrid films increases the activation energy. And the greater the PTS content, the higher the activation energy obtained in hybrid films.

The service lifetimes of pure PI and PI/PSSQ-like hybrid films with different conversion levels and service temperatures are shown in Figures 4, 5, 6 and Table IV. Service temperature and lifetime of the

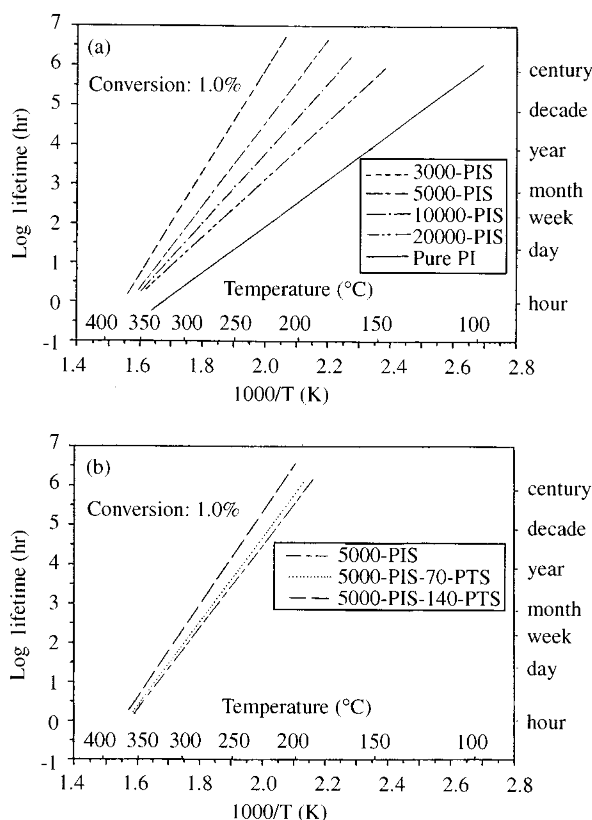


Figure 4. Service lifetime of (a) pure PI and X-PIS, (b) 5000-PIS-y-PTS with 1% conversion.

PI films are the function of molecular block chain length and PSSQ-like content. The service lifetime increases with decreasing PI block chain length in X-PIS films and also increases with PTS content in X-PIS-y-PTS. The best thermal lifetime based on a 5 % weight loss is over 1.5 months at 350 °C; over 16 years at 300 °C, and over 200 years at 250 °C for 3000-PIS and 5000-PIS-140-PTS films. The thermal lifetime of 3000-PIS and 5000-PIS-140-PTS is 70 times greater than that of pure PI at 350 °C, 400 times greater at 300 °C and 2000 times greater at 250 °C. The X-PIS and X-PIS-y-PTS films promote the Ea and lifetime significantly. They can also promote the service temperature.

In summary, the decomposition activation energy of PI/PSSQ-like hybrid films becomes higher and service lifetime longer as the PI chain length shortens and the PTS content increases. Increasing the APTS content resulted in a shorter PI chain length and a higher crosslinking density. In addition, a higher PTS content represents a higher inorganic silica content and better thermal properties of the material. Therefore, increasing the APTS and PTS content will enhance the Ea and service lifetime.

Figure 7 shows the dynamic storage modulus

**Table IV.** Service lifetime (hr) of the PI, X-PIS and X-PIS-y-PTS hybrid films with different conversiion levels and service temperatures.

| Temperature / Conversion (wt%) / Sample code | 250 °C | | | 300 °C | | | 350 °C | | |
|---|---|---|---|---|---|---|---|---|---|
| | 1% | 2.5% | 5% | 1% | 2.5% | 5% | 1% | 2.5% | 5% |
| 3000-PIS | $5.5 \times 10^4$ | $3.7 \times 10^5$ | $2.3 \times 10^7$ | $3.7 \times 10^2$ | $3.2 \times 10^3$ | $1.4 \times 10^5$ | 4.9 | 58 | $1.2 \times 10^3$ |
| 5000-PIS | $4.2 \times 10^3$ | $1.4 \times 10^5$ | $3.2 \times 10^6$ | 68 | $1.6 \times 10^3$ | $2.7 \times 10^4$ | 2.5 | 33 | $3.3 \times 10^2$ |
| 10000-PIS | $7.0 \times 10^2$ | $4.6 \times 10^4$ | $1.0 \times 10^6$ | 32 | $6.3 \times 10^2$ | $1.6 \times 10^4$ | 2.0 | 22 | $2.0 \times 10^2$ |
| 20000-PIS | $3.0 \times 10^2$ | $6.5 \times 10^3$ | $8.0 \times 10^4$ | 19 | $2.0 \times 10^2$ | $2.2 \times 10^3$ | 1.5 | 12 | 72 |
| Pure PI | 26 | $2.3 \times 10^2$ | $9.5 \times 10^3$ | 3.0 | 17 | $3.3 \times 10^2$ | 0.4 | 1.9 | 17 |
| 5000-PIS-70-PTS | $5.5 \times 10^3$ | $2.3 \times 10^5$ | $2.3 \times 10^7$ | 85 | $2.5 \times 10^3$ | $5.3 \times 10^4$ | 3.0 | 43 | $5.5 \times 10^2$ |
| 5000-PIS-140-PTS | $2.0 \times 10^4$ | $5.8 \times 10^5$ | $2.7 \times 10^7$ | $2.4 \times 10^2$ | $4.6 \times 10^3$ | $1.5 \times 10^5$ | 4.2 | 72 | $1.3 \times 10^3$ |

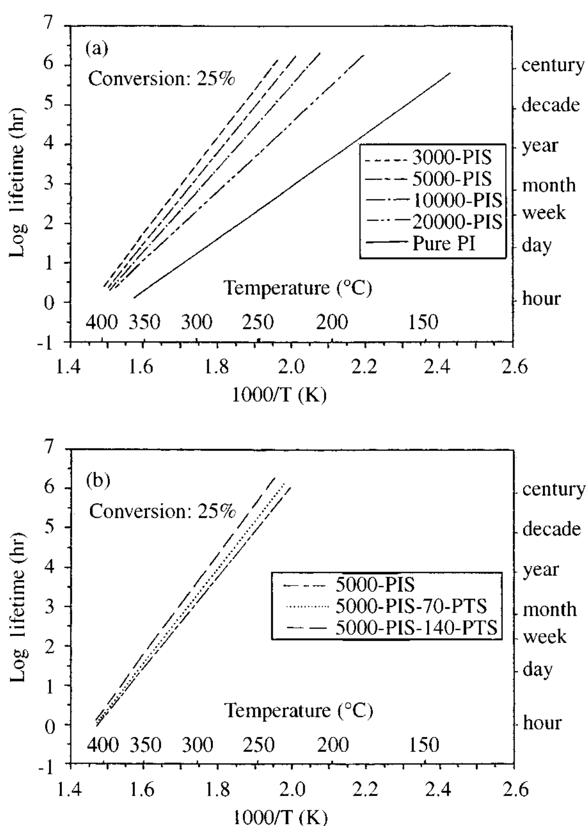


**Figure 5.** Service lifetime of (a) pure PI and X-PIS, (b) 5000-PIS-y-PTS with 2.5% conversion.

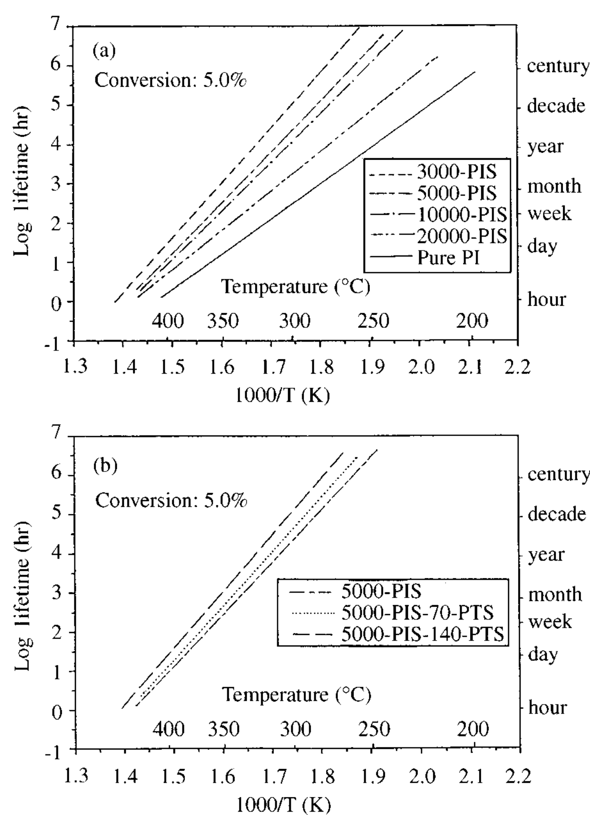


**Figure 6.** Service lifetime of (a) pure PI and X-PIS, (b) 5000-PIS-y-PTS with 5% conversion.

as a function of temperature for 5000-PIS and 5000-PIS-100-PTS at frequencies of 0.1, 0.5, 1, 5, 10 and 20 Hz. The shifting of the storage modulus curves to higher temperatures with increasing frequency occurs in accordance with the time-temperature superposition. Figure 8 shows the logarithmic storage modulus of 5000-PIS around the glass transition region against the logarithmic frequency (rad/sec) at different temperatures. It reveal that the storage modulus is a function of frequency and temperature. The data column on the extreme left represents data collected at 0.1 Hz, while that on the extreme right represents data collected at 20 Hz. Material on the extreme top represents data collected at the low temperature 242 °C, while on that the extreme bottom represents data collected at the high temperature 302 °C. After measurement, Pure PI, 3000-PIS, 10000-PIS, 15000-PIS, 20000-PIS, 5000-PIS-24-PTS, 5000-PIS-50-PTS, 5000-PIS-100-PTS, and 10000-PIS-100-PTS films have similar behaviors.

The shift factors $a_T$ calculated from the data of Figure 8 and the graphical fitting of the WLF (Williams-Landel-Ferry) equation are shown in Figure 9. The WLF equation is predicted as [38,42].

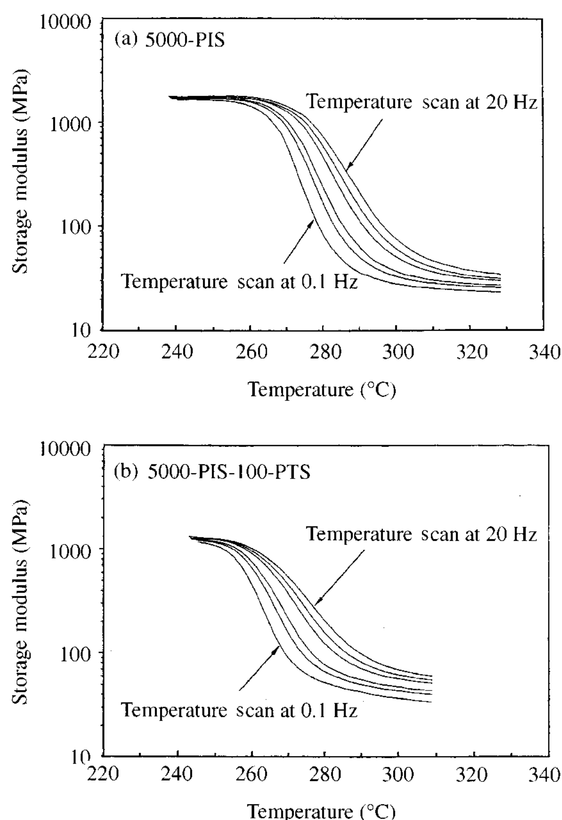


**Figure 7.** Dynamic storage modulus as a function of temperature for (a) 5000-PIS, (b) 5000-PIS-100-PTS at various frequencies: 0.1, 0.5, 1, 5, 10, 20 Hz.

$$\mathrm{Log}\, a_T = \frac{-C_1(T-T_0)}{C_2+(T-T_0)} \qquad (2)$$

$T_o$ is a reference temperature. $a_T$ is the shift factor. Values of $a_T$ at different temperatures ($T_g$−10 > T > $T_g$+30~40) can be calculated from the above equation. Figure 9 shows the $C_1$ and $C_2$ characteristic constants of the WLF equation of pure PI, 5000-PIS, 5000-PIS-100-PTS, 10000-PIS, 10000-PIS-100-PTS and the glass transition temperature ($T_g$) as a reference temperature ($T_0$). After testing, all other 3000-PIS, 15000-PIS, 20000-PIS, 5000-PIS-24-PTS, and 5000-PIS-50-PTS films follow the WLF equation, in which the $C_1$ and $C_2$ are 4.9-7.5 and 40.0-52.2, respectively. The shift factor $a_T$ is the ratio of the relaxation time at temperature T and the relaxation time at $T_g$. The expected shift factors are practically identical with those obtained from modulus relaxation (Figure 8).

Figure 10 shows the logarithmic relaxation modulus (E') curves of 5000-PIS hybrid film as a function of logarithmic frequency at 250, 260, 270, 280, 290 and 300 °C, respectively. The relaxation modulus increases with the frequency at constant temperatures. As expected, at the same frequency,

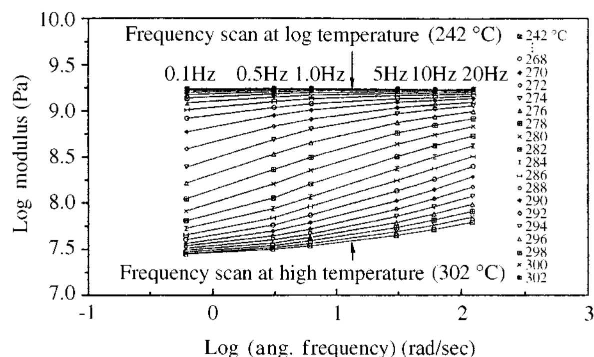


**Figure 8.** Storage modulus of 5000-PIS in the glass transition region plotted against frequency at different temperatures as indicated.

the relaxation modulus decreases with temperature. At the same relaxation modulus, the relaxation frequency increases with the temperature. Other PI/PSSQ-like films also exhibit a similar behavior. Figure 11 displays the logarithmic relaxation time of 5000-PIS films as a function of temperatures at different relaxation modulus log E' = 7.5, 8.0, 8.5 and 9.0 Pa. It shows the relaxation times of the film depending on the relaxation modulus and temperature. The figure indicates that the criteria of higher relaxation modulus and temperature leads to a decrease in the relaxation time; that is, higher modulus and temperature levels lower the relaxation time. Curves of the relaxation time versus temperature follow the same trend.

The master curves from the storage modulus data for pure ODA-ODPA polyimide and X-PIS films are exhibited in Figure 12. All these curves show the effect of frequency on the modulus of hybrid films corresponding to the reference temperature of 280 °C. At very low frequencies (corresponding to long relaxation times) a low modulus behaves similar to a rubber. In contrast, at high frequencies (corresponding to short relaxation times) all the films have a high modulus. The dynamic mechanical relaxation data can be fitted to a single smooth master curve. These master curves demonstrate that data collected over only 0.1 to 20 Hz of frequency can be transformed to cover eleven to thirteen orders of frequency. Figure 12 also illustrates the a phenomenon that the shorter the polyimide block chain length, the higher the storage modulus, whether at low frequency (corresponding to a long relaxation time or high temperature response) or at high frequency (corresponding to a short relaxation time or low temperature response). The X-PIS hybrid films with shorter PI block chain lengths have a higher crosslinking density [14] and it, in turn, leads to a higher modulus. Figure 13 shows the logarithmic

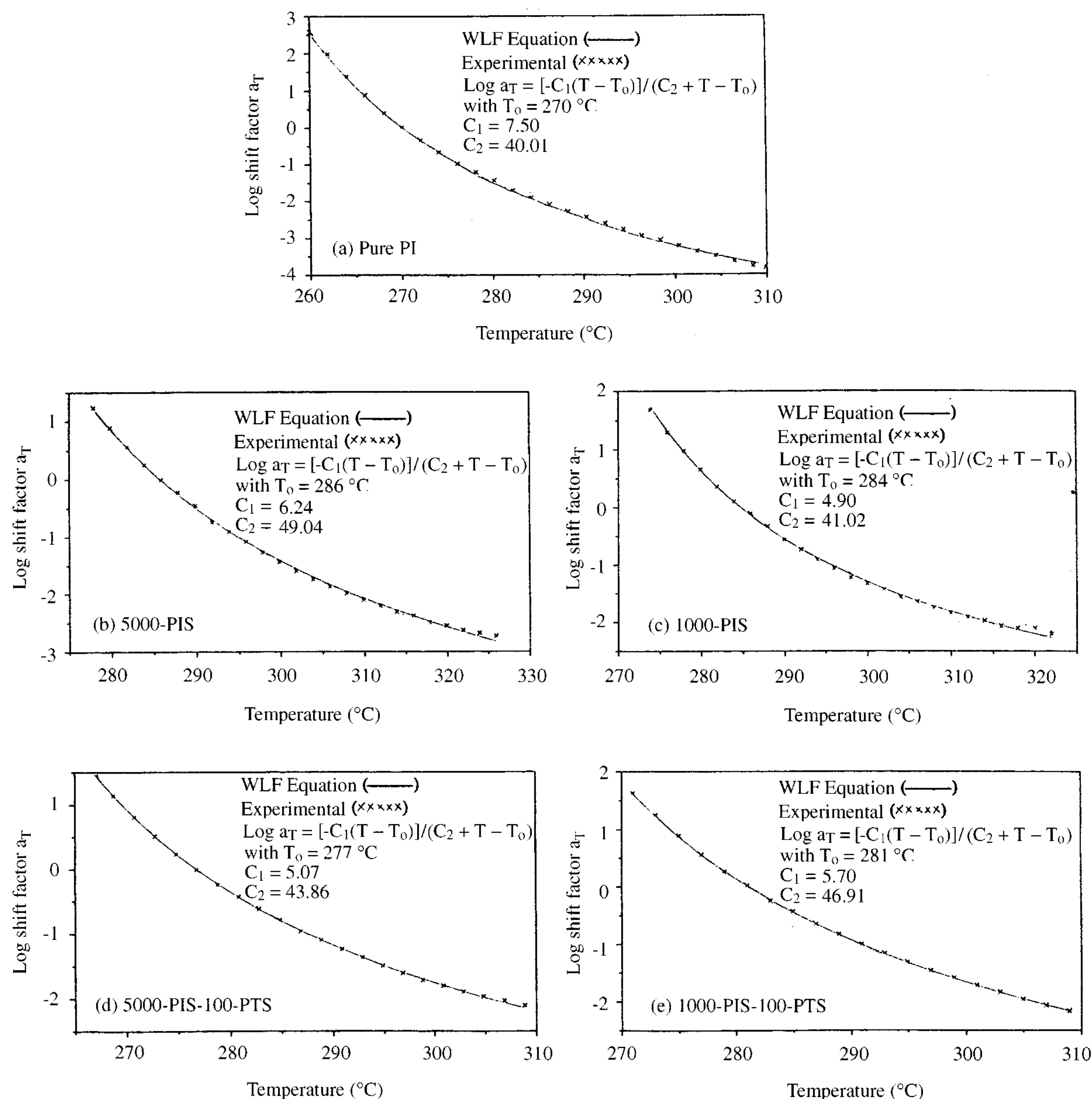


**Figure 9.** Temperature dependence of the shift factor $a_T$ for (a) pure PI, (b) 5000-PIS, (c) 10000-PIS, (d) 5000-PIS-100-PTS, and (e) 10000-PIS-100-PTS. (Equation $T_g$ is used as the reference temperature)

relaxation time curves of pure ODA-ODPA polyimide and X-PIS hybrid films as a function of temperatures at a constant relaxation modulus log E' = 8.5 Pa. It shows the relationship between temperatures, relaxation times and compositions. At the relaxation modulus of log E' = 8.5 Pa, X-PIS films have a longer relaxation time than pure PI. When the reference temperature is 250 °C, lower than the glass transition temperatures of both types of films, the relaxation time of 3000-PIS is 30 times that of pure PI. If the reference temperature is 280 °C near $T_g$, the relaxation time of 3000-PIS is 800 times greater than that of pure PI. This is attributed to the terminal APTS, which leads to a network PSSQ-like component in the polyimide structure which promotes the modulus and high temperature lifetime of the PI films.

In order to compare the characteristics of X-PIS and X-PIS-y-PTS films, master curves of 10000-PIS and 10000-PIS-100-PTS films are shown in Figure 14. These two curves have been referred to a temperature of 280 °C. Both 10000-PIS and 10000-PIS-100-PTS films have a constant PI block chain length. The latter introduces PTS into the 10000-PIS structure to form a greater PSSQ-like domain [14]. It has been found that the density of the films

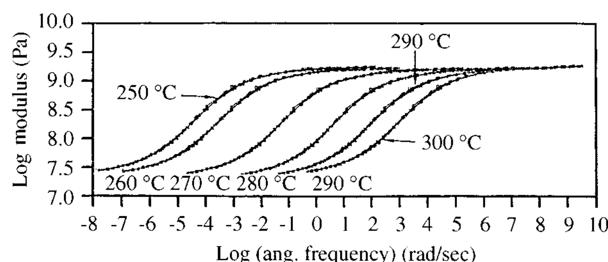


**Figure 10.** Logarithmic relaxation modulus curves as a function of logarithmic frequency for 5000-PIS at various temperatures : 250, 260, 270, 280, 290 and 300 °C.

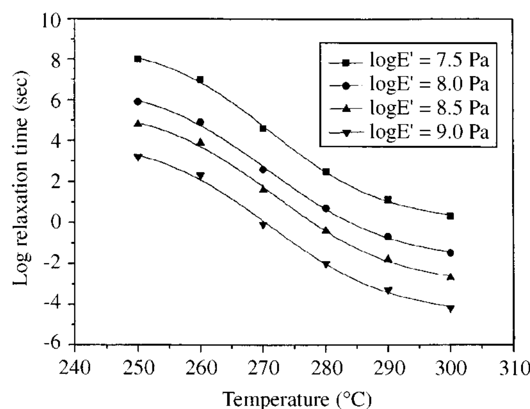


**Figure 11.** Logarithmic relaxation time as function of temperature for 5000-PIS at various logarithmic relaxation modulus: 7.5, 8.0, 8.5, 9.0 Pa.

decreases with the PTS content, and the room temperature modulus also decreases with the PTS content [13,14]. In Figure 14, at a higher frequency (> $10^2$ rad/sec) the relaxation modulus of 10000-PIS-100-PTS film is lower than that of 10000-PIS film. However, at a lower frequency (< $10^2$ rad/sec), the former is higher than that of 10000-PIS. There is a cross point at a frequency of around $10^2$ rad/sec. The decrease of relaxation modulus in the transition region is more significant in 10000-PIS film than in 10000-PIS-100-PTS film. The greater PSSQ-like crosslink domain decreases the chain movement more effectively during the transition period. In frequency-temperature superposition, this property at higher frequency corresponds to that at a lower temperature, and at a lower frequency it corresponds to that at a higher temperature. Therefore, at lower temperatures (below $T_g$), the modulus of X-PIS-y-PTS is lower than of X-PIS, but the former is higher than the latter at relatively higher temperatures (above $T_g$). Figure 15 shows the curves of logarithmic relaxation time of 5000-PIS and 5000-PIS-100-PTS, and 10000-PIS and 10000-PIS-100-PTS hybrid films as a function of temperature. Figure 15(a) displays the relaxation time at a relatively higher modulus ($5\times10^8$ Pa) and Figure 15(b) the relaxation time at a lower modulus ($5\times10^7$ Pa). Figure 15(a) shows that the 5000-PIS and 10000-PIS have the longer relaxation time (lifetime) than the corresponding 5000-PIS-100-PTS and 10000-PIS-100-PTS. However, with the increase in temperature, the relaxation times of X-PIS and the corresponding X-PIS-100-PTS become closer. In our previous publications [13,14], we reported that X-PIS-y-PTS films have a relatively lower $T_g$ than the corresponding X-PIS films. X-PIS films have a higher relaxation time than X-PIS-y-PTS films at $5\times10^8$ Pa, a modulus below $T_g$; in Figure 15(b), the X-PIS-100-PTS films have a longer relaxation time than the corresponding X-PIS films at $5\times10^7$ Pa, a modulus above $T_g$. When the temperature is 260 °C, the relaxation times of 5000-PIS-100-PTS and 10000-PIS-100-PTS are 2.5 times that of the corresponding 5000-PIS and 10000-PIS films, respectively. However, at 300 °C, the relaxation times of 5000-PIS-100-PTS and 10000-PIS-100-PTS films are 60 times and 10 times that of the corresponding 5000-PIS and 10000-PIS films, respectively. The X-PIS-y-PTS films show a higher relaxation time at the modulus of $5\times10^7$ Pa than that of X-PIS and pure PI film at higher temperatures. Table V shows the relaxation times of 5000-PIS, 5000-PIS-24-PTS, 5000-PIS-50-PTS and 5000-PIS-100-PTS hybrid films as a function of temperature and relaxation modulus (i.e., $5\times10^7$ Pa and $5\times10^8$ Pa). It confirms that the relaxation time decreases along with PTS content at 260-300 °C at the modulus $5\times10^8$ Pa, but the lifetime increases along with the PTS content at the modulus $5\times10^7$ Pa. This can be attributed to the greater PSSQ-like domain size or composition in the structure. The crosslink structure PSSQ-like component decreases the PI molecule chain movement and endures structural disintegration.

## Conclusion

This study contributes to an understanding of the lifetime of PI/PSSQ-like hybrid films by TGA and DMA. The results show that PI/PSSQ-like hybrid films have longer lifetimes than pure ODA-ODPA polyimides. In the TGA decomposition kinetic study of X-PIS films, the decomposition activation energy, service lifetime, and service temperature increase with the shortening PI block length in the hybrid films primarily because the PI block bonds chemically with the APTS, leading to a network structure and a high temperature lifetime. In the series of X-PIS-y-PTS films with a constant PI block

**Figure 12.** Master curves of pure ODA-ODPA polyimide, X-PIS. (Reference temperature = 280 °C)

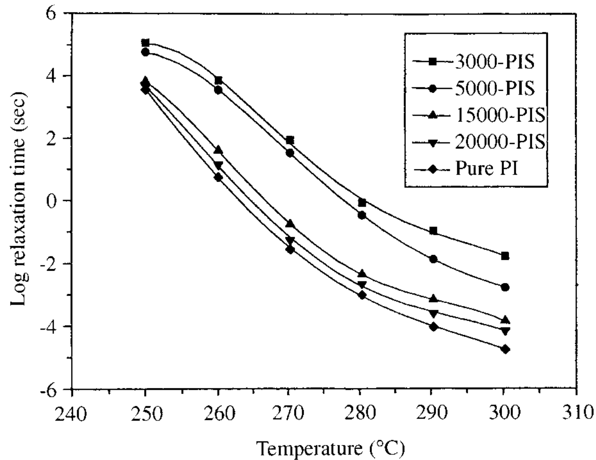


**Figure 13.** Logarithmic relaxation time curves of pure ODA-ODPA polyimide and X-PIS hybrid films as a function of temperature. (Logarithmic relaxation modulus = 8.5 Pa)

length, the decomposition activation energy, service lifetime and service temperature increase with the PTS content. Introducing more PTS content into X-PIS promotes high temperature performance and long-term stability.

In the DMA dynamic mechanical relaxation study, evaluation of the data indicates that the behavior of the PI/PSSQ-like around the glass transition temperature follows the WLF equation and a smooth master curve can be obtained. The viscoelastic characteristics of the hybrid films at a specific temperature can be predicted over a broad time scale using the WLF equation through the shift factor $a_T$. In the series of X-PIS hybrid films, shortening the PI block chain length increases the relaxation modulus of master curves at the same frequency and re-

**Table V.** Relaxation time (sec) of 5000-PIS and 5000-PIS-y-PTS hybrid films with different relaxation modulus and temperatures.

| Sample code / E' (Pa)[a] / Temperature (°C) | 5000-PIS | | 5000-PIS-24-PTS | | 5000-PIS-50-PTS | | 5000-PIS-100-PTS | |
|---|---|---|---|---|---|---|---|---|
| | $5 \times 10^8$ | $5 \times 10^7$ | $5 \times 10^8$ | $5 \times 10^7$ | $5 \times 10^8$ | $5 \times 10^7$ | $5 \times 10^8$ | $5 \times 10^7$ |
| 260 | $3.2 \times 10^3$ | $7.9 \times 10^5$ | $1.0 \times 10^3$ | $1.3 \times 10^6$ | $2.5 \times 10^2$ | $1.6 \times 10^6$ | 13 | $2.0 \times 10^6$ |
| 270 | 10 | $3.2 \times 10^3$ | 4.0 | $5.0 \times 10^3$ | 1.3 | $6.3 \times 10^3$ | 0.13 | $1.0 \times 10^4$ |
| 280 | 0.1 | 4.0 | $5.0 \times 10^{-2}$ | 79 | $3.2 \times 10^{-2}$ | $1.3 \times 10^{-2}$ | $1.3 \times 10^{-2}$ | $3.2 \times 10^2$ |
| 290 | $4.0 \times 10^{-3}$ | 0.1 | $3.2 \times 10^{-3}$ | 2.5 | $2.5 \times 10^{-3}$ | 6.3 | $1.6 \times 10^{-3}$ | 40 |
| 300 | $7.9 \times 10^{-4}$ | 0.25 | $7.9 \times 10^{-4}$ | 0.63 | $6.3 \times 10^{-4}$ | 2.0 | $5.0 \times 10^{-4}$ | 16 |

(a) Relaxation modulus.

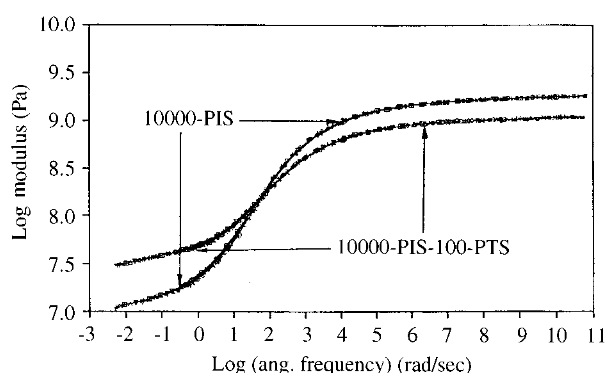


**Figure 14.** Master curve of 10000-PIS and 10000-PIS-100-PTS. (Reference temperature = 280 °C)

sults from the higher crosslinking density, which leads to a strong network structure and the astricition of movement of the chain at high temperatures. In the series of X-PIS-y-PTS films with a constant PI block chain length, introducing PTS into the X-PIS structure causes the relaxation modulus to decrease at a relatively higher frequency (> $10^2$ rad/sec), which corresponds to a lower temperature (below $T_g$), but the relaxation modulus increase at a relatively lower frequency (<$10^2$ rad/sec), corresponding to a higher temperature (above $T_g$). The relaxation time of X-PIS-y-PTS films decreases with a PTS content at the modulus $5\times10^8$ Pa, but increases with a PTS content at the modulus $5\times10^7$ Pa, which corresponds to the higher temperature relaxation modulus. That means that a higher PTS content enhances the high temperature relaxation modulus and relaxation time of the X-PIS-y-PTS films. The X-PIS-y-PTS also have a longer lifetime than X-PIS and pure PI at higher temperatures. Therefore, it is concluded that at high temperatures the PI/PSSQ-like hybrid films are more reliable in their thermal and mechanical properties than pure ODA-ODPA polyimide.

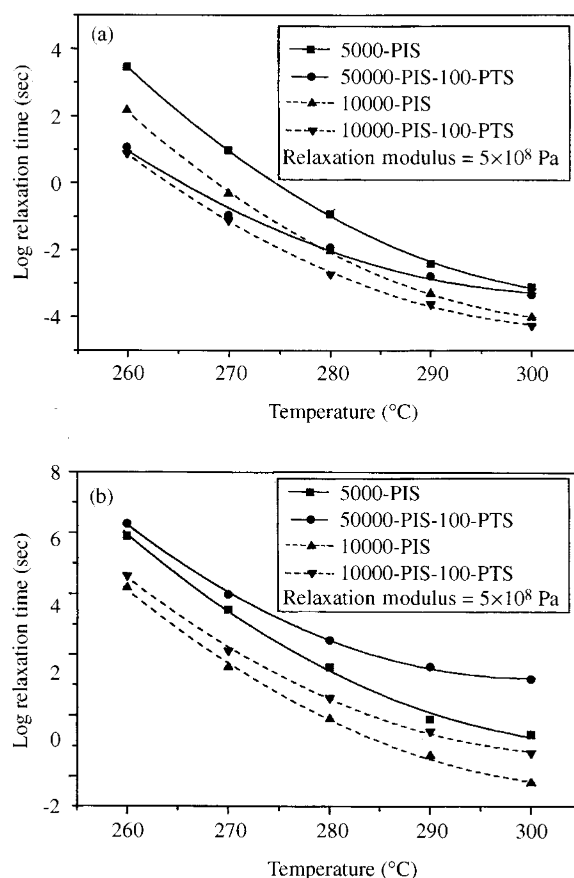


**Figure 15.** Logarithmic relaxation time curves of 5000-PIS and 5000-PIS-100-PTS, 10000-PIS and 10000-PIS-100-PTS hybrid films as a function of temperature. (a) relaxation modulus = $5\times10^8$ Pa (b) relaxation modulus = $5\times10^7$ Pa.

## Acknowledgments

The authors would like to express their appreciation to the National Science Council of the Republic of China for financial support for this study under grant NSC 89-2216-E009-024.

## Reference


1. D. Wilson, H. D. Stenzenberger and P. M. Hergenrother, Eds., *Polyimides*, New York, Blackie, p. 227, 1990.
2. M. K. Ghosh and K. L. Mittal, Eds., *Polyimides: Fundamentals and Applications*, New York, Marcel Dekker, 1996.
3. K. L. Mittal, *Polyimides: Synthesis, Characterization, and Applications*, New York, Plenum Press, 1984.
4. J. M. Abadie and B Sillion, Eds., *Polyimids and other High-Temperaturre Polymers*, New York, Elsevier, 1991.
5. S. Ukishima, M. Iijima, M. Sato, Y. Takahashi and E. Fukada, *Thin Solid Films*, **308**, 475 (1997).
6. G. Hougham, G. Tesoro and J. Shaw, *Macromolecules*, **27**, 3462 (1994).
7. G. Hougham, G. Tesoro and A. Viehbeck, *Macromolecules*, **29**, 3453 (1996).
8. G. Hougham, G. Tesoro, A. Viehbeck and J. D. Chapple-Sokol, *Macromolecules*, **27**, 5964 (1994).
9. Y. Y. Maruo, Y. Andoh and S. J. Sasaki, *Vac. Sci. Technol.*, **11**, 2590 (1993).
10. J.L. Hedrick, H. J. Cha, R. D. Miller, D. Y. Yoon, H. R. Brown, S. Srinivasan, Pietro. R. Di, R. F. Cook, J. H. Hummel, D. P. Klaus, E. G. Liniger and E. E. Simonyi, *Macromolecules*, **30**, 8512 (1997).
11. W. C. Chen, S. C. Lin, B. T. Dai and M. S. Tsai, *J. Electrochem. Soc.*, **146**, 3004 (1999).
12. W. C. Chen and C. T. Yen, *J. Polym. Res.*, **6**, 197 (1999).
13. M. H. Tsai and W. T. Whang, *J. Appl. Polym. Sci.*, Accepted, to be published.
14. M. H. Tsai, W. T. Whang, *Polymer*, **42**, 4197 (2001).
15. Y. Iyoku, M. Kakimoto and Y. Imai, *High Performance Polym.*, **6**, 43 (1994).
16. Y. Iyoku, M. Kakimoto and Y. Imai, *High Performance Polym.*, **6**, 53 (1994).
17. Y. Iyoku, M. Kakimoto and Y. Imai, *High Performance Polym.*, **6**, 95 (1994).
18. L. Mascia and A. Kioul, *Polymer*, **36**, 3649 (1995).
19. S. A. Srinivasan, L. J. Hedrick, R. D. Miller and Pietro. R Di, *Polymer*, **38**, 3129 (1997).
20. S. Wang, Z. Ahmad and J. H. Mark, *Macromol. Reports*, **A31**, 411 (1994).
21. S. Wang, Z, Ahmad and J. E. Mark, *Polym. Bull.*, **31**, 323 (1993).
22. A. Morikawa, Y. Iyoku, M. Kakimoto and Y. Imai, *J. Mater. Chem.*, **2**, 679 (1992).
23. A. Morikawa, Y. Iyoku, M. Kakimoto and Y. Imai, *Polym. J.*, **24**, 107 (1992).
24. Z. Ahmad, M. I. Sarwar and J. E. Mark, *J. Mater. Chem.*, **7**, 259 (1997).
25. A. Kioul and L. Mascia, *J. Non-Cryst. Solids*, **175**, 169 (1994).
26. S. Wang, Z. Ahmad and J. E. Mark, *Chem. Mater.*, **6**, 943 (1994).
27. J. Wen, G. L. Wilkes, *Chem. Mater.*, **8**, 1667 (1996).
28. M. Nandi, J. A. Conklin, L. Salvatijr and A. Sen, *Chem Mater.*, **3**, 201 (1991).
29. L. Mascia and A. J. Kioul, *Mater. Sci. Lett.*, **13**, 641 (1994).
30. J. H. Flynn and L. A. Wall, *Polym. Lett.*, **4**, 323 (1966).
31. N. Regnier and C. Guibe, *Polym. Degrad. Stabil.*, **55**, 165 (1997).
32. Y. D. Moon and Y. M. Lee, *J. Appl. Polym. Sci.*, **50**, 1461 (1993).
33. P. P. Huo and P. Cebe, *Polymer*, **34**, 696 (1993).
34. C. Marais, G. Villoutreix, *J. Appl. Polym. Sci.*, **69**, 1983 (1998).
35. C. G. Robertson, J. E. Monat and G. L. Wilkes, *J. Polym. Sci., Polym. Phys.*, **37**, 1931 (1999).
36. D. R. Veazie and T. S. Gates, *Exp. Mech.*, **37**, 62 (1997).
37. A. Lee, *High Performance Polym.*, **8**, 475 (1996).
38. J. D. Ferry, *Viscoelastic Properties of Polymers.*, 3 rd Ed., New York, Wiley, 1980.
39. L. E. Nielsen, *Mechanical Properties of Polymers and Composites*, Vol. **2**, New York, Marcel Dekker, 1974.
40. I. M. Ward and D. W. Hadleg, Eds., *An Introduction to The Mechanical Properties of Solid Polymer*, New York, John Wiley and Sons, 1993.
41. T. E. Murayama, *Dynamic Mechanical Analysis of Polymeric Material*, New York, Elsevier, 1978.
42. M. L. Williams, R. F. Landel and J. D. Ferry, *J. Amer. Chem. Soc.*, **77**, 3701 (1955).